A Fast Reduced-Order Model for the Full-Wave FEM Analysis of Lossy Inhomogeneous Anisotropic Waveguides

Francesco Bertazzi, Oscar Antonio Peverini, Michele Goano, *Member, IEEE*, Giovanni Ghione, *Senior Member, IEEE*, Renato Orta, *Senior Member, IEEE*, and Riccardo Tascone

***Abstract*—The evaluation of the frequency response of waveguiding structures by means of the full-wave finite-element method requires solving a large generalized eigenvalue problem for each frequency. This paper describes a novel approach, based on the singular-value decomposition, which drastically reduces the order of the eigenvalue problem. By inspection of the singular values, the accuracy level of the procedure may be controlled. The technique is applied to the analysis of open and closed waveguides with arbitrary cross section, lossy conductors, and anisotropic dielectric layers, by means of vector elements of generic order; higher order elements are shown to allow the accurate evaluation of fields inside lossy conductors with fewer unknowns, besides exactly modeling normal field discontinuities at material interfaces. Examples of application of the reduced-order technique are shown concerning both non-TEM and quasi-TEM structures.**

***Index Terms*—Finite-element method, higher order vector elements, reduced-order models, singular-value decomposition.**

I. Introduction

THE design of microwave, millimeter-wave, and opto-electronic circuits requires the accurate characterization of complex, sometimes unconventional, waveguiding structures. The analysis technique must be able to deal with arbitrary cross sections, anisotropic substrates with dielectric losses, and metallic regions of finite conductivity whose thickness may be smaller or larger than the skin penetration depth within the frequency band of interest. Moreover, both the fundamental and higher order modes have to be characterized. Finally, some opto-electronic applications require the optical and microwave field distributions to be evaluated in order to compute their superposition integral.

Among suitable analysis techniques, the finite-element method (FEM) probably is the most general. Besides allowing for arbitrary nonplanar geometries and dielectric and magnetic anisotropic materials, the method enables to accurately estimate conductor losses beyond the skin-effect approximation by direct discretization of field-penetrated conductor layers. After choosing a suitable basis function set, application of Galerkin's procedure to the vector wave equation yields a large (but sparse) generalized eigenvalue problem for each frequency to be solved for the propagation constant. The use of higher order elements usually helps reducing the number of unknowns at the expense of the problem sparsity; besides, higher order elements are able to correctly describe the discontinuity of the normal field components at the interfaces between different materials.

If the solution over a given band is sought, then the analysis must be repeated for many frequency sampling points in the range of interest, with a very high computational burden. Fast frequency-sweep methods based on model reduction, first developed for the analysis of large linear(-ized) circuits [1], [2], have been applied with success to the analysis of electromagnetic (EM) devices. For example, in [3], Padé-via-Lanczos, Krylov, and rational Krylov methods are used to obtain the scattering parameters of EM devices, in [4] and [5], the asymptotic waveform evaluation (AWE) method is implemented in conjunction with the FEM and with the method of moments (MoM), respectively and in [6], the complex frequency-hopping technique is adopted to obtain time- and frequency-domain solutions of EM problems. Concerning the modal analysis of dielectric waveguides, a fast frequency-sweep technique, based on a tangential-vector FEM combined with the AWE, is reported in [7].

Recently, a novel technique to generate a reduced set of problem-matched basis functions has been introduced with application to MoM analysis of frequency-selective surfaces [8]. The numerical generation of such basis functions is based on the MoM solution of the scattering problem for a selected set of values of a variable parameter. In this paper, a fast numerical technique for spectral-response computations of an arbitrary two-dimensional waveguide, based on the full-wave finite-element method (FW-FEM) in conjunction with this novel approach, is presented. To the authors' knowledge, the concept of problem-matched basis functions has never been applied to guided-wave problems. Moreover, the method introduced in [8] is extended to extract additional information from the frequency derivatives of the solution.

The paper is structured as follows. In Section II, the waveguiding problem is formulated using three field components of the electric field. Section III presents the reduced-order model. The key point is the numerical generation of a reduced set of entire-domain problem-matched basis functions, derived as linear combinations of the original local basis functions. This problem-matched basis functions set is extremely efficient in

Manuscript received July 2, 2001; revised January 8, 2002. This work was supported in part by the Italian National Research Council (CNR) under the MADESS II Project.

F. Bertazzi, M. Goano, G. Ghione, and R. Orta are with the Dipartimento di Elettronica, Politecnico di Torino, I-10129 Turin, Italy (e-mail: ghione@polito.it).

O. A. Peverini and R. Tascone are with the Istituto di Ricerca sull'Ingegneria delle Telecomunicazioni (IRITI-CNR), Politecnico di Torino, I-10129 Turin, Italy.

Publisher Item Identifier 10.1109/TMTT.2002.802323.

representing the solution at least on the frequency range of interest, thus drastically reducing the CPU time required to evaluate the frequency response. In Section IV, the accuracy and computational advantages (CPU time reduction of about one order of magnitude) of the reduced-order model are shown through a series of examples. Some concluding remarks are finally presented in Section V.

II. Full-Wave FEM Analysis

We consider a lossy anisotropic waveguide with an arbitrary cross section Ω. From Maxwell's equations, the following vectorial wave equation is derived:

$$\nabla \times \left([\nu]\nabla \times \vec{E}\right) - k^2[\tilde{\epsilon}_r]\vec{E} = 0 \tag{1}$$

where $k = \omega^2\epsilon_0\mu_0$ is the free-space wavenumber, $[\nu] = [\mu_r]^{-1}$, and $[\tilde{\epsilon}_r] = [\epsilon_r] - j[\sigma]/(\omega\epsilon_0)$. The relative permittivity and permeability tensors $[\epsilon_r]$, $[\mu_r]$ are assumed to be diagonal. Dielectric and conductor losses are included in the imaginary part of the permittivity tensor. Assuming for all of the field components a z-dependence of the form $\exp(-j\gamma z)$, with $\gamma = \beta - j\alpha$ as the complex propagation constant and dividing the waveguide cross section Ω into a number of hybrid interpolation-type triangular functions, we expand the electric field within each element as

$$\begin{aligned}\vec{E} =& E_x\hat{x} + E_y\hat{y} + E_z\hat{z} \\ =& \left(\hat{x}\{\boldsymbol{U}\}^T + \hat{y}\{\boldsymbol{V}\}^T\right)\cdot\{\boldsymbol{E}_t\}\exp(-j\gamma z) \\ &+ j\gamma\hat{z}\{\boldsymbol{N}\}^T\cdot\{\boldsymbol{E}_z\}\exp(-j\gamma z)\end{aligned} \tag{2}$$

where $\{\boldsymbol{E}_t\}$ and $\{\boldsymbol{E}_z\}$ are, respectively, the transverse- and longitudinal-variable vectors for each element, $\{\boldsymbol{U}\}$ and $\{\boldsymbol{V}\}$ are the basis functions' vectors for the triangular curl-conforming element, and $\{\boldsymbol{N}\}$ is the basis functions' vector for the triangular nodal element.

Curl-conforming bases that ensure the continuity of tangential-field components at element interfaces and eliminate spurious modes in finite-element formulations were first introduced by Nedelec [9]. Recently, higher order interpolatory forms of both curl- and divergence-conforming vector bases have been presented [10]. Curl-conforming bases complete to order p are obtained by forming the product of the zeroth-order curl-conforming bases with polynomial factors complete to pth order. We use multiplying polynomials of shifted interpolatory form. It must be noticed that, since $\nabla_t \times \vec{E}_t$ and $\nabla_t E_z$ should be complete to the same order p, the transverse vector component of the electric field $\vec{E}_t$ must be represented by curl-conforming functions of order p and the longitudinal expansion functions have to be of order $p+1$ [11]. Higher order elements can correctly model the discontinuity of the normal field components at interfaces between different materials. The correct behavior of the field component normal to the triangle edges cannot be described by zeroth-order bases because such functions do not have interior degrees of freedom. For $p = 1$, each triangular element contributes with only two interior degrees of freedom, whereas the element has three edges. For $p = 2$, there are six interior degrees of freedom per triangle and, hence, the normal field discontinuity (or continuity) at each element edge can be modeled [12], [13].

Application of Galerkin's procedure to the vectorial wave (1) yields the following $N \times N$ linear sparse eigenvalue problem [14], [15]:

$$\begin{pmatrix}\boldsymbol{K}_{tt} & \boldsymbol{0}\\ \boldsymbol{0} & \boldsymbol{0}\end{pmatrix}\cdot\begin{pmatrix}\boldsymbol{E}_t\\ \boldsymbol{E}_z\end{pmatrix} = \gamma^2\begin{pmatrix}\boldsymbol{M}_{tt} & \boldsymbol{M}_{tz}\\ \boldsymbol{M}_{zt} & \boldsymbol{M}_{zz}\end{pmatrix}\cdot\begin{pmatrix}\boldsymbol{E}_t\\ \boldsymbol{E}_z\end{pmatrix} \tag{3}$$

which is written for convenience as

$$\left(\boldsymbol{K} - \gamma^2\boldsymbol{M}\right)\cdot\boldsymbol{E} = \boldsymbol{0} \tag{4}$$

with

$$\boldsymbol{K}(k) = \boldsymbol{K}_0 + k\boldsymbol{K}_1 + k^2\boldsymbol{K}_2 \tag{5}$$

$$\boldsymbol{M}(k) = \boldsymbol{M}_0 + k\boldsymbol{M}_1 + k^2\boldsymbol{M}_2. \tag{6}$$

The Dirichlet boundary conditions are applied by eliminating all the rows and columns corresponding to the variables associated to interpolating points lying on electric walls. The Neumann boundary conditions at magnetic walls need not to be explicitly enforced since they are natural boundary conditions for the formulation adopted. The final generalized eigenvalue problem is solved with the function `sptarn` of the MATLAB partial differential equations (PDEs) toolbox, based on the implicitly restarted Arnoldi method as implemented in ARPACK [16]. (The most recent and efficient techniques for the solution of sparse eigenvalue problems are discussed in [17], where URL's to available implementations are also presented.)

III. Reduced-Order Model

The FEM formulation of the modal problem for waveguiding structures corresponds to the solution of the generalized eigenvalue problem (4). If one deals with a large-size problem and is looking for the solution over a wide frequency band, then the analysis can become very time consuming. In order to speed up computations, the AWE technique can be adopted. The matrices $\boldsymbol{K}$ and $\boldsymbol{M}$, eigenvalues $\lambda = \gamma^2$, and eigenvectors $\boldsymbol{E}$ are all functions of the wavenumber k. Substituting their Taylor expansions around $k = k_0$ into (4) and matching the coefficients of the corresponding powers of $(k - k_0)$, a recursive system of equations to be solved for the qth-order frequency derivatives (moments) $\{\lambda^{(q)}(k_0), \boldsymbol{E}^{(q)}(k_0)\}_{q=1}^{d}$ is obtained [7]. Since all linear systems have the same coefficient matrix, the computation of the eigenvector derivatives can be performed efficiently once a factorization of this matrix is available. After the frequency moments have been obtained, λ and $\boldsymbol{E}$ may be expressed over a frequency range around a specified expansion point k_0 with their Taylor expansions. It is well known, however, that power series always have a finite radius of convergence in the presence of poles. Padé approximations, instead, employ rational functions to approximate a function also beyond the convergence region of its Taylor expansion. To obtain a wide-band response, several reduced-order models are usually combined together in a piecewise fashion to form a single reduced-order model across the band of interest. Unfortunately, higher order moments are usually scarcely linearly independent so that their explicit use, as in AWE, can result in ill-conditioned numerical computations [1].

In order to overcome the numerical instability due to the explicit use of the frequency moments and to extract information from multiple points, we propose a novel approach.

Let $\{\boldsymbol{E}_j(k_i)\}_{i,j}$ with $j=1,\ldots,M$ and $i=1,\ldots,P$ be M modal eigenvectors of (4) computed at P frequency points. The set of vectors $\{\boldsymbol{E}_j(k_i)\}_{i,j}$ define a reduced-order subspace Ξ of the original Hilbert space

$$\Xi=\bigcup_{i=1}^{P}\operatorname{span}\Big\{\boldsymbol{E}_1(k_i),\ldots,\boldsymbol{E}_M(k_i)\Big\}. \tag{7}$$

The basis vectors in (7) define a subspace Ξ containing $\boldsymbol{E}(k)$, but one has to decide how many of them are necessary. If too few basis vectors are chosen, there is an unacceptable loss of accuracy in the representation of $\boldsymbol{E}(k)$. If too many are selected, one has a redundant description and some basis vectors may be linearly dependent. In order to define an orthonormal basis of Ξ and its dimension, vectors $\{\boldsymbol{E}_j(k_i)\}_{i,j}$ are arranged columnwise in a matrix $\boldsymbol{X}$ of dimension $N\times L$ [where $L=MP$ and N is the number of unknowns in (4)], which is subjected to the economy-size (thin) singular-value decomposition (SVD) [18]

$$\boldsymbol{X}=\boldsymbol{T}\cdot\boldsymbol{S}\cdot\boldsymbol{R}^{\dagger} \tag{8}$$

where $\boldsymbol{T}$ is an $N\times L$ matrix, $\boldsymbol{S}$ is an $L\times L$ diagonal matrix with positive elements (singular values), $\boldsymbol{R}$ is an $L\times L$ unitary matrix, and $\dagger$ stands for complex conjugate and transpose. The columns of $\boldsymbol{T}$ are the left singular vectors. The significance of the various singular vectors in the description of the modal fields is measured by the amplitude of the corresponding singular values. Since those typically range over several orders of magnitude, not all of the singular vectors are needed for accuracy. Moreover, by inspection of the dynamic range of the singular values, the accuracy level of the procedure can be controlled. A small dynamic range means that the corresponding singular vectors do not have sufficient span to adequately represent $\boldsymbol{E}(k)$.

Let $Q\le L$ be the number of singular vectors assumed to be adequate to span the subspace Ξ. These singular vectors define a set of orthogonalized problem-matched basis functions of the reduced-order subspace. The projection of the global matrices onto the subspace Ξ yields the reduced-order model

$$\left(\tilde{\boldsymbol{K}}-\gamma^2\tilde{\boldsymbol{M}}\right)\cdot\tilde{\boldsymbol{E}}=0 \tag{9}$$

with

$$\tilde{\boldsymbol{K}}=\boldsymbol{T}_Q^{\dagger}\cdot\boldsymbol{K}\cdot\boldsymbol{T}_Q \tag{10}$$

$$\tilde{\boldsymbol{M}}=\boldsymbol{T}_Q^{\dagger}\cdot\boldsymbol{M}\cdot\boldsymbol{T}_Q \tag{11}$$

where $\boldsymbol{T}_Q$ consists of the first Q columns of matrix $\boldsymbol{T}$. The new eigenvalue equation to be solved for each frequency value has size $Q\times Q$, where Q may be much smaller than N. Notice that, owing to (5) and (6), the system matrices in (9) can be assembled directly in the reduced-order representation. Equation (9) can be inexpensively solved by a direct method and the approximate eigenvectors of (4) may be computed via the matrix–vector product

$$\boldsymbol{E}=\boldsymbol{T}_Q\cdot\tilde{\boldsymbol{E}}. \tag{12}$$

In order to extract more information from the solution in the expansion points k_i, the qth-order frequency derivatives of the eigenvectors $\{\boldsymbol{E}^{(q)}(k_i)\}_{i,q}$ may be computed up to the order D. For simplicity, we discuss the extension of the reduced-order model for a single mode of the structure. The set of vectors $\{\boldsymbol{E}^{(q)}(k_i)\}_{i,q}$ define a reduced-order subspace Ξ of the original Hilbert space

$$\Xi=\bigcup_{i=1}^{P}\operatorname{span}\Big\{\boldsymbol{E}^{(0)}(k_i),\ldots,\boldsymbol{E}^{(D)}(k_i)\Big\}. \tag{13}$$

Once again, the SVD yields an orthonormalized set of basis functions. As the order of the derivatives is increased, the numerical evaluation of the frequency moments becomes less accurate [19], but unlike the explicit moment-matching AWE procedure, the current approach provides a numerically stable reduction model. In contrast with the subspace defined in (7), the vectors $\{\boldsymbol{E}^{(q)}(k_i)\}_{i,q}$ are now not homogeneous and the selection of the singular vectors cannot be based on the dynamics of the corresponding singular values. In the following examples, whenever frequency derivatives have been computed, all the singular vectors have been retained in the reduced-order model.

IV. Results

The convergence properties of higher order elements and the accuracy of the reduced-order model are discussed through a series of examples including isotropic and anisotropic, lossless and lossy inhomogeneous waveguides. All computations were performed with MATLAB on a PC equipped with 1 GB of RAM.

A. Dielectric-Loaded Waveguide

As a first numerical example, we consider a rectangular waveguide with metallic walls loaded with a dielectric slab, as shown in the inset of Fig. 1(a). Analytical solutions are known for this type of structure [20] and they can be used to investigate the convergence properties of higher order elements. The relative error affecting the propagation constant of the fundamental LSE_{10} mode has been computed as a function of the number of unknowns, for different orders of the interpolatory elements. As expected, higher order bases achieve faster convergence rates [see Fig. 1(b)]. However, it must be remarked that improved convergence properties are obtained at the expense of producing less sparse system matrices. For this reason, elements of order higher than three are rarely used in practice.

The proposed fast frequency-sweep technique has been applied to the dominant mode of the waveguide. In order to investigate the numerical accuracy of this technique, the residual error is defined as

$$\mathcal{E}=\frac{\|\boldsymbol{K}(k)\cdot\boldsymbol{E}(k)-\lambda(k)\boldsymbol{M}(k)\cdot\boldsymbol{E}(k)\|}{\|\boldsymbol{E}(k)\|} \tag{14}$$

where $\boldsymbol{E}(k)$ and $\lambda(k)$ are the approximate eigenpairs obtained from (9) and (12). In Fig. 2, we compare the error introduced by two different reduced-order models. In the first model (solid line), the reduced representation has been obtained computing the solution at $P=4$ frequency points. In the second model (dashed line), the frequency derivatives of the solution have

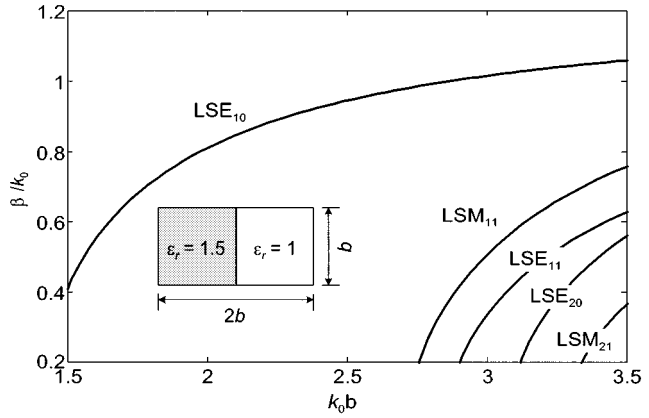

(a)

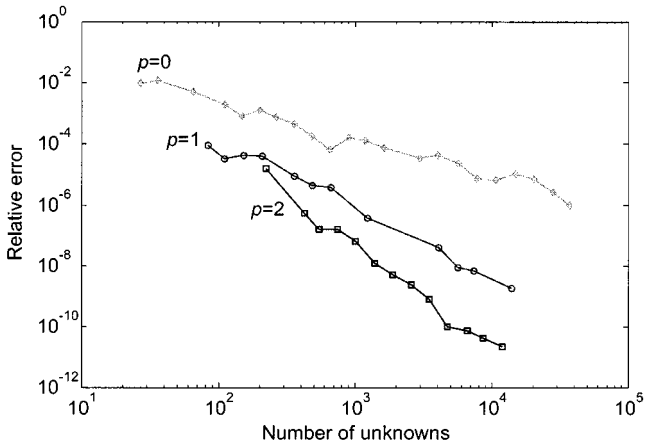

(b)

Fig. 1. (a) Dispersion characteristics of the lowest five modes in the dielectric-slab-loaded rectangular waveguide shown in the inset. (b) Relative error affecting the propagation constant of the fundamental LSE_{10} mode (at the normalized frequency $k_0 b = 3$) for different orders ($p = 0, 1, 2$) of the curl-conforming elements as a function of the number of unknowns.

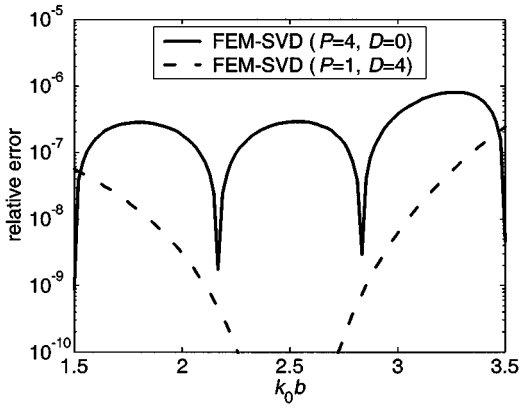

Fig. 2. Relative error introduced by two different reduced-order models versus frequency for the dominant mode of the structure.

been computed up to the order $D = 4$ at a single expansion point $k_0 b = 2.5$. In both cases, all the singular vectors have been retained. The computation of the exact solution in 50 frequency points through the direct application of the FEM procedure takes 80 s, while reduced-order models lower the CPU times to 12 and 6.4 s, respectively. The computational domain has been divided into 62 triangles and basis elements of order $p = 2$ have been employed.

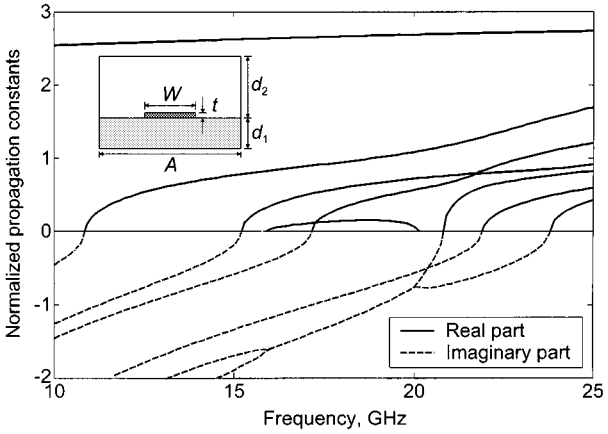

Fig. 3. Normalized dispersion diagram for a box microstrip line on an isotropic substrate ($\epsilon_r = 8.875$). The dimensions of the waveguide are $A = 12.7$ mm, $d_1 = 1.27$ mm, $d_2 = 11.43$ mm, $W = 1.27$ mm, and $t = 0.127$ mm.

B. Microstrip Line

In the following example, we consider a shielded microstrip transmission line on an isotropic lossless substrate, as sketched in the inset of Fig. 3. The strip is assumed to be a perfect conductor. The goal of this example is to demonstrate that the FEM–SVD technique is able to predict multimode characteristics. Fig. 3 shows the propagation constants (normalized with respect to the wavenumber k) of the first seven even modes of the structure versus frequency. The eigenvectors have been evaluated at $P = 8$ frequency points, evenly spaced in the band of interest from 10 to 25 GHz. The application of the SVD decomposition yields 50 singular vectors. The range of the singular values is approximately ten orders of magnitude, which confirms that the frequency sampling rate is sufficient to represent the modal solutions of the guiding structure. In order to eliminate the redundancy from the basis functions set, the 23 singular vectors corresponding to singular values five order of magnitude below the dominant one have been neglected. As it can be observed from Fig. 3, the selected problem-matched basis functions alone are sufficient to reproduce the dispersion diagram of the structure with excellent accuracy (see [21, Fig. 3] and [15, Fig. 3.8]). Even if the waveguide is lossless, the propagation constants of the modes may be complex, as discussed in [15]. The sixth and seventh modes degenerate into two complex-conjugate modes and then split again into two ordinary modes. This phenomenon is correctly described by the reduced-order model, proving that the present method has a broad range of applicability.

For a given accuracy, the equivalent dimension Q of the subspace Ξ depends on the complexity of the spectral response over the frequency range of interest. However, the number of elements in the computational domain Ω and their order p does not affect Q.

C. Coplanar Waveguide (CPW)

In Fig. 4, we sketch the cross section of a symmetric CPW. This structure is a typical RF line for electrooptical (EO) mod-

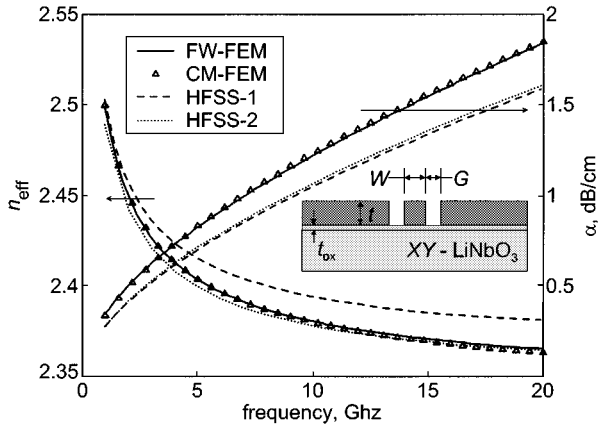

Fig. 4. Microwave effective index $n_{\rm eff}$ and attenuation $\alpha_{\rm dB}$ (dB/cm) of a symmetric CPW on an X-cut $LiNbO_3$ substrate with a thin SiO_2 buffer layer, computed with FW-FEM (solid lines), CM-FEM (triangles), and HFSS (dashed lines: 15 000 tetrahedra; dotted lines: 50 000 tetrahedra).

ulators on $LiNbO_3$ substrates [22]. In such applications, synchronous coupling with the optical signal is usually achieved by inserting a low-dielectric-constant buffer layer underneath the electrodes and by increasing the electrode thickness. Moreover, the line-to-ground spacing must be kept small to maximize the coupling between the microwave and optical fields. Due to the small gap width, these lines exhibit high losses, which can be minimized through electrode shape design. Owing to their complex cross section and their need for optimization, coplanar lines for EO modulators are typical candidates for analysis and design with FEM-based EM computer-aided design (CAD) tools.

Fig. 4 shows the computed propagation and attenuation constants of a symmetric CPW on an X-cut Y-propagating $LiNbO_3$ substrate (the relative permittivities are 43 and 28 perpendicular and parallel to the substrate surface, respectively) coated with a 1-μm-thick SiO_2 buffer layer ($\epsilon_r = 3.90$). The gold ($\sigma = 4.1 \times 10^7$ S/m) electrode thickness t is 20 μm. The central electrode width W is 10 μm and the ground-plane gap G is 20 μm. The loss tangents of the $LiNbO_3$ substrate and SiO_2 buffer layer are $\tan\delta_s = 0.004$ and $\tan\delta_{ox} = 0.016$, respectively [23]. The results of this approach are compared with version 7.0.11 of HFSS, a commercial three-dimensional (3-D) FEM simulator,[1] and with a numerical conformal mapping analysis coupled with quasi-TEM FEM (CM-FEM) [24], [25].

In contrast with pertubative methods based on the skin-effect approximation, the computational domain of FW-FEM includes the electrodes, which are characterized by their complex dielectric constants. Our FW-FEM computations have been carried out on a coarse mesh with 984 triangles, taking advantage of the symmetry of the structure. Elements of order $p = 2$ have been used, resulting in an eigenvalue problem with 14 130 unknowns. The reduced-order model has been obtained computing the frequency moments of the solution up to the order $D = 4$ at $P = 2$ expansion points, $f = 1$ GHz, and $f = 20$ GHz. The agreement between our FW-FEM and CM-FEM is excellent over the entire frequency range. Two sets of HFSS results are also shown, computed with 15 000 and 50 000 tetrahedra, respectively (the latter case is close to the limit that may be handled on a computer with 1 GB of RAM). The HFSS propagation constant is close to our FW-FEM results in both cases and the differences become negligible when the denser mesh is used. On the other hand, HFSS underestimates losses with respect to CM-FEM and our FW-FEM and only a slight increase is seen with the denser mesh. Since the same discrepancy can be observed with *in vacuo* CPWs (where numerical conformal mapping (CM) results are virtually exact), we deem that it may be related to an insufficient refinement of the HFSS mesh close to the metallic edges.

[1]HFSS is a registered trademark of the Ansoft Corporation, Pittsburgh, PA.

TABLE I
CONTRIBUTIONS TO THE TOTAL CPU TIME

	Order p	CPU time, s
matrix	0	2.5
assembly	1	8
process	2	40
zeroth-order	0	1.6
moments	1	16
(each frequency)	2	87
higher-order	0	1
moments	1	11
(each frequency)	2	71
SVD	0	1
and	1	5
matrix products	2	14
reduced-order sweep	any	negligible
Total FEM	0	$2.5 + 1.6 \times 20 = 34.5$
	1	$8 + 16 \times 20 = 328$
	2	$40 + 87 \times 20 = 1780$
Total FEM-SVD	0	$2.5 + (1.6 + 1) \times 2 + 1 = 8.7$
	1	$8 + (16 + 11) \times 2 + 5 = 67$
	2	$40 + (87 + 71) \times 2 + 14 = 370$

Table I reports all the different contributions to the total CPU time for the direct and reduced-order FEM, with the only exception of the mesh generation time, measured on a PC equipped with an 800-MHz Intel Pentium III processor. An overall comparison is also provided for a frequency sweep over 20 samples on a 20-GHz interval.[2]

Due to their layered structure, CPWs cannot carry pure TEM modes. Therefore, the concept of characteristic impedance does not apply to CPWs in a rigorous sense. However, this quantity is very useful for design purposes. Among all the possible formulations, we refer to the widely used power–current definition [14]

$$Z_c = \frac{2\mathcal{P}}{|I|^2} \tag{15}$$

[2]In our opinion, it would be unfair to compare the timings of our reduced-order FW-FEM with HFSS, which is a 3-D simulator. As a matter of fact, the computation of a 20-point frequency sweep with HFSS required approximately 3 h with the 15 000-tetrahedron grid and approximately one day with the 50 000-tetrahedron grid on the same computer used for FW-FEM simulations.

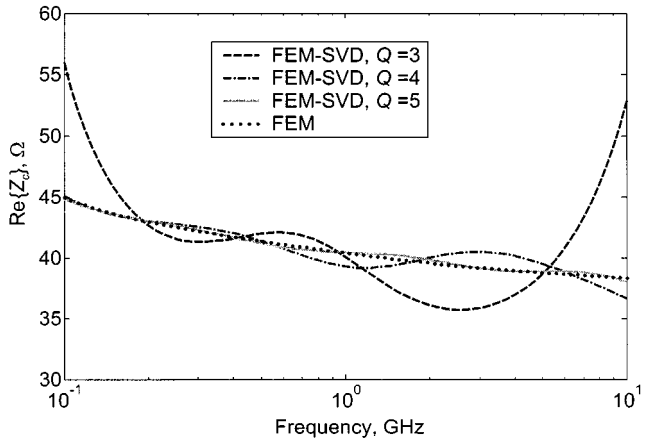

(a)

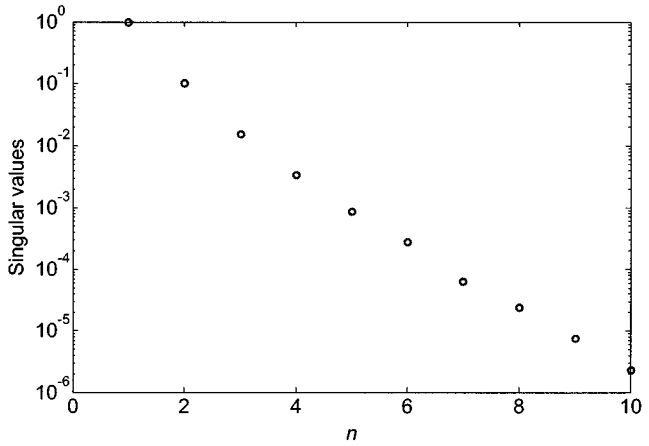

(b)

Fig. 5. (a) Characteristic impedance $Z_c(\Omega)$ of the CPW of Fig. 4 versus frequency computed with the FEM at each frequency point and via the reduced-order method with $Q = 3, 4, 5$ problem-matched basis functions. (b) Normalized singular values for $n = 1, \ldots, 10$.

where $\mathcal{P}$ is the modal power and I is the total z-directed current carried by the central electrode. $\mathcal{P}$ and I are related to the eigenvectors of (9) by

$$\mathcal{P} = \frac{1}{2}\frac{\gamma^*}{\omega\mu_0}\left(\tilde{\boldsymbol{E}}^T \cdot \tilde{\boldsymbol{M}}_{tt}^* \cdot \tilde{\boldsymbol{E}}^* + \tilde{\boldsymbol{E}}^T \cdot \tilde{\boldsymbol{M}}_{tz}^* \cdot \tilde{\boldsymbol{E}}^*\right) \quad (16)$$

$$I = j\gamma\sigma\left(\boldsymbol{N}^T \cdot \boldsymbol{T}_{Q,z}\right) \cdot \tilde{\boldsymbol{E}} \quad (17)$$

with

$$\boldsymbol{N} = \sum_e \int\int_e \{\boldsymbol{N}\} dxdy \quad (18)$$

where $\boldsymbol{T}_{Q,z}$ is the lower part of $\boldsymbol{T}_Q$, relative to the longitudinal variables, $\tilde{\boldsymbol{M}}_{tt}$ and $\tilde{\boldsymbol{M}}_{tz}$ are the projections onto the subspace Ξ of matrices $\boldsymbol{M}_{tt}$ and $\boldsymbol{M}_{tz}$, respectively, σ is the electrode conductivity, $\{\boldsymbol{N}\}$ is the scalar shape functions vector defined in (2), and the summation $\sum_e$ extends over the elements on the central electrode.

Fig. 5(a) shows the real part of characteristic impedance evaluated using Q problem-matched basis functions. The eigenvectors of (4) have been computed at $P = 10$ frequency points evenly spaced in the band of interest from 0.1 to 10 GHz. The range of the singular values is approximately six orders of magnitude [see Fig. 5(b)], which confirms that the frequency sampling rate is sufficient to represent the solution. As can be observed, five problem-matched basis functions are able to capture the EM field behavior of the structure with excellent accuracy. This is possible, despite the fact that, owing to skin-effect losses, the internal field distribution in the conductors drastically changes within the selected frequency range. The dependence of the subspace Ξ on the particular problem under consideration does not enable the definition of general criteria relating Q and the error $\mathcal{E}$; however, as a rule-of-thumb, basis functions corresponding to singular values at least three orders of magnitude below the dominant one can be safely neglected.

V. Conclusion

A novel fast frequency-sweep technique has been described, which enables to efficiently evaluate, through a vector FEM-based approach, the propagation characteristics of inhomogeous anisotropic lossy quasi-TEM/non-TEM waveguides. Speed improvements of about one order of magnitude with respect to traditional approaches in the wide-band analysis of typical structures have been demonstrated. Besides being computationally efficient, the fast sweep technique is robust and allows a self-consistent automatic monitoring of the accuracy. The examples discussed demonstrate the applicability of the proposed method to a variety of structures; in particular, for quasi-TEM lines, it has been shown that the method also allows for the efficient computation of the characteristic impedance.

Acknowledgment

The authors are indebted to V. Niculae, Dipartimento di Elettronica, Politecnico di Torino, Turin Italy, for useful discussions.

References

[1] P. Feldmann and R. W. Freund, "Efficient linear circuit analysis by Padé approximation via the Lanczos process," *IEEE Trans. Computer-Aided Design*, vol. 14, pp. 639–649, May 1995.

[2] E. Gad and M. Nakhla, "Model reduction for DC solution of large nonlinear circuits," in *IEEE/ACM Int. CAD Conf.*, San Jose, CA, Nov. 1999, pp. 376–379.

[3] T. Zhou, S. L. Dvorak, and J. L. Prince, "Application of subspace projection approaches for reduced-order modeling of electromagnetic systems," in *IEEE 8th Elect. Performance Electron. Packag. Topical Meeting* , San Diego, CA, Oct. 1999, pp. 89–92.

[4] C. J. Reddy, M. D. Deshpande, C. R. Cockrell, and F. B. Beck, "Fast RCS computation over a frequency band using method of moments in conjunction with asymptotic waveform evaluation technique," *IEEE Trans. Antennas Propagat.*, vol. 46, pp. 1229–1233, Aug. 1998.

[5] J. Gong and J. L. Volakis, "AWE implementation for electromagnetic FEM analysis," *Electron. Lett.*, vol. 32, no. 24, pp. 2216–2217, Nov. 1996.

[6] M. A. Kolbehdari, M. Srinivasan, M. S. Nakhla, Q. J. Zhang, and R. Achar, "Simultaneous time and frequency domain solutions of EM problems using finite element and CFH techniques," *IEEE Trans. Microwave Theory Tech.*, vol. 44, pp. 1526–1534, Sept. 1996.

[7] S. V. Polstyanko, R. Dyczij-Edlinger, and J.-F. Lee, "Fast frequency sweep technique for the efficient analysis of dielectric waveguides," *IEEE Trans. Microwave Theory Tech.*, vol. 45, pp. 1118–1126, July 1997.

[8] C. K. Aanandan, P. Debernardi, R. Orta, R. Tascone, and D. Trinchero, "Problem-matched basis functions for moment method analysis—An application to reflection gratings," *IEEE Trans. Antennas Propagat.*, vol. 48, pp. 35–40, Jan. 2000.

[9] J. C. Nedelec, "Mixed finite elements in R^3," *Numer. Math.*, vol. 35, no. 3, pp. 315–341, 1980.
[10] R. D. Graglia, D. R. Wilton, and A. F. Peterson, "Higher order interpolatory vector bases for computational electromagnetics," *IEEE Trans. Antennas Propagat.*, vol. 45, pp. 329–342, Mar. 1997.
[11] J.-F. Lee, D.-K. Sun, and Z. J. Cendes, "Full-wave analysis of dielectric waveguides using tangential vector finite elements," *IEEE Trans. Microwave Theory Tech.*, vol. 39, pp. 1262–1271, Aug. 1991.
[12] P. Savi, R. D. Graglia, G. Ghione, and M. Pirola, "Full-wave FEM analysis of lossy anisotropic waveguides," in *Int. Electromagn. Adv. Applicat. Conf.*, Turin, Italy, Sept. 1999, pp. 201–204.
[13] P. Savi, I.-L. Gheorma, and R. D. Graglia, "Full-wave high-order FEM model for lossy anisotropic waveguides," *IEEE Trans. Microwave Theory Tech.*, vol. 50, pp. 495–500, Feb. 2002.
[14] M. Koshiba, Y. Tsuji, and M. Nishio, "Finite-element modeling of broad-band traveling-wave optical modulators," *IEEE Trans. Microwave Theory Tech.*, vol. 47, pp. 1627–1633, Sept. 1999.
[15] G. Pelosi, R. Coccioli, and S. Selleri, *Quick Finite Elements for Electromagnetic Waves*. Norwood, MA: Artech House, 1998.
[16] R. B. Lehoucq, D. C. Sorensen, and C. Yang, *ARPACK Users' Guide: Solution of Large-Scale Eigenvalue Problems with Implicitly Restarted Arnoldi Methods*. Philadelphia, PA: SIAM, 1998.
[17] Z. Bai, J. Demmel, J. Dongarra, A. Ruhe, and H. van der Vorst, Eds., *Templates for the Solution of Algebraic Eigenvalue Problems: A Practical Guide*. Philadelphia, PA: SIAM, 2000.
[18] G. H. Golub and C. F. Van Loan, *Matrix Computations*, 3rd ed. Baltimore, MD: The John Hopkins Univ. Press, 1996.
[19] X.-M. Zhang and J.-F. Lee, "Application of the AWE method with the 3-D TVFEM to model spectral responses of passive microwave components," *IEEE Trans. Microwave Theory Tech.*, vol. 46, pp. 1735–1741, Nov. 1998.
[20] R. E. Collin, *Field Theory of Guided Waves*. New York: McGraw-Hill, 1960.
[21] L. Valor and J. Zapata, "Efficient finite element analysis of waveguides with lossy inhomogeneous anisotropic materials characterized by arbitrary permittivity and permeability tensors," *IEEE Trans. Microwave Theory Tech.*, vol. 43, pp. 2452–2459, Oct. 1995.
[22] N. Dagli, "Wide-bandwidth lasers and modulators for RF photonics," *IEEE Trans. Microwave Theory Tech.*, vol. 47, pp. 1151–1171, July 1999.
[23] K. Noguchi, H. Miyazawa, and O. Mitomi, "Frequency-dependent propagation characteristics of coplanar waveguide electrode on 100 GHz Ti:$LiNbO_3$ optical modulator," *Electron. Lett.*, vol. 34, no. 7, pp. 661–663, Apr. 1998.
[24] F. Carbonera, F. Bertazzi, M. Goano, and G. Ghione, "Accurate and efficient numerical quasi-TEM modeling of coplanar waveguides for high-speed electro-optic modulators," in *Opt. Soc. Amer. Integrated Photon. Res. Tech. Dig.*, Monterey, CA, June 2001, pp. ITuI2-1–ITuI2-3.
[25] ——, "Efficient CM-FEM modeling of coplanar waveguides for high-speed E/O modulators," in *GAAS 2001*, London, U.K., pp. 607–610.

Francesco Bertazzi received the Laurea degree in electronics engineering from the Politecnico di Torino, Turin, Italy in 2000, and is currently working toward the Ph.D. degree in electronics engineering at the Politecnico di Torino.

His research is focused on the application of the FEM to waveguiding problems.

Oscar Antonio Peverini was born in Lisbon, Portugal, in 1972. He received the Laurea degree (*summa cum laudae*) in telecommunications engineering and Ph.D. degree in electronics engineering from the Politecnico di Torino, Turin, Italy, in 1997 and 2001, respectively.

From August 1999 to March 2000, he was a Visiting Member with the Applied Pysics/Integrated Optics Department, University of Paderborn, Paderborn, Germany. In February 2001, he joined the Istituto di Ricerca sull'Ingegneria delle Telecomunicazioni e dell'Informazione (IRITI), a newly established institute of the Italian National Council (CNR), Politecnico di Torino. Since December 2001, he has been a Researcher with the IRITI. His research interests include numerical simulation and design of surface acoustic wave (SAW) waveguides and interdigital transducers (IDTs) for integrated acoustooptical devices and microwave passive components.

Michele Goano (M'98) received the Laurea and Ph.D. degrees in electronics engineering from the Politecnico di Torino, Turin, Italy in 1989 and 1993, respectively.

In 1994 and 1995, he was a Post-Doctoral Fellow with the Département de Génie Physique, École Polytechnique de Montréal, Montréal, QC, Canada. In 1996, he joined the faculty of the Dipartimento di Elettronica, Politecnico di Torino. He was a Visiting Scholar with the School of Electrical and Computer Engineering, Georgia Institute of Technology, Atlanta, and with the Department of Electrical and Computer Engineering, Boston University, Boston, MA. He is currently involved in research on coplanar components, optical modulators, and wide-bandgap semiconductor devices.

Giovanni Ghione (M'87–SM'94) received the Laurea degree in electronics engineering from the Politecnico di Torino, Torino, Italy, in 1981.

From 1983 to 1987, he was a Research Assistant with the Politecnico di Torino. From 1987 to 1990, he was an Associate Professor with the Politecnico di Milano, Milan, Italy. In 1990 he joined the University of Catania, Catania, Italy, as Full Professor of electronics. Since 1991, he has been a Full Professor with the II Faculty of Engineering, Politecnico di Torino. Since 1981, he has been engaged in Italian and European research projects (ESPRIT 255, COSMIC and MANPOWER) in the field of active and passive microwave CAD. His current research interests concern the physics-based simulation of active microwave and opto-electronic devices, with particular attention to noise modeling, thermal modeling, and active device optimization. His research interests also include several topics in computational electromagnetics, including coplanar component analysis. He has authored or coauthored over 150 papers and book chapters in the above fields.

Prof. Ghione is member of the Associazione Elettrotecnica Italiana (AEI). He is an Editorial Board member of the IEEE TRANSACTIONS ON MICROWAVE THEORY AND TECHNIQUES.

Renato Orta (M'92–SM'99) received the Laurea degree in electronics engineering from the Politecnico di Torino, Turin, Italy, in 1974.

Since 1974, he has been a member of the Department of Electronics, Politecnico di Torino, initially as an Assistant Professor, then as an Associate Professor and, since 1999, as a Full Professor. In 1985, he was a Research Fellow with the European Space Research and Technology Center (ESTEC–ESA). Noordwijk, The Netherlands. In 1998, he was a Visiting Professor (CLUSTER Chair) with the Technical University of Eindhoven, Eindhoven, The Netherlands. He currently teaches courses on EM field theory and optical components. His research interests include the areas of microwave and optical components, radiation and scattering of EM and elastic waves, and numerical techniques.

Riccardo Tascone was born in Genoa, Italy, in 1955. He received the Laurea degree in electronics engineering from the Politecnico di Torino, Turin, Italy, in 1980.

From 1980 to 1982, he was with the Centro Studi e Laboratori Telecomunicazioni (CSELT), Turin, Italy, where he was mainly involved with frequency-selective surfaces, waveguide discontinuities, and microwave antennas. In 1982, he joined the Centro Studi Propagatione e Antenne (CESPA), Turin, Italy, a laboratory of the Italian National Research Council (CNR), where he was initially a Researcher and, since 1991, a Senior Scientist (Dirigente di Ricerca). He is currently the Head of the Applied Electromagnetics Section, Istituto di Ricerca sull'Ingeneria delle Telecomunicazioni e dell'Informazione (IRITI), Politecnico di Torino, a newly established institute of the CNR. He has held various teaching positions in the area of electromagnetics with the Politecnico di Torino. His current research activities concern the areas of microwave antennas, dielectric radomes, frequency-selective surfaces, radar cross section, waveguide discontinuities, microwave filters, multiplexers, and optical passive devices.